Polymer Chemistry

Accepted Manuscript

ROYAL SOCIETY OF CHEMISTRY

www.rsc.org/polymers

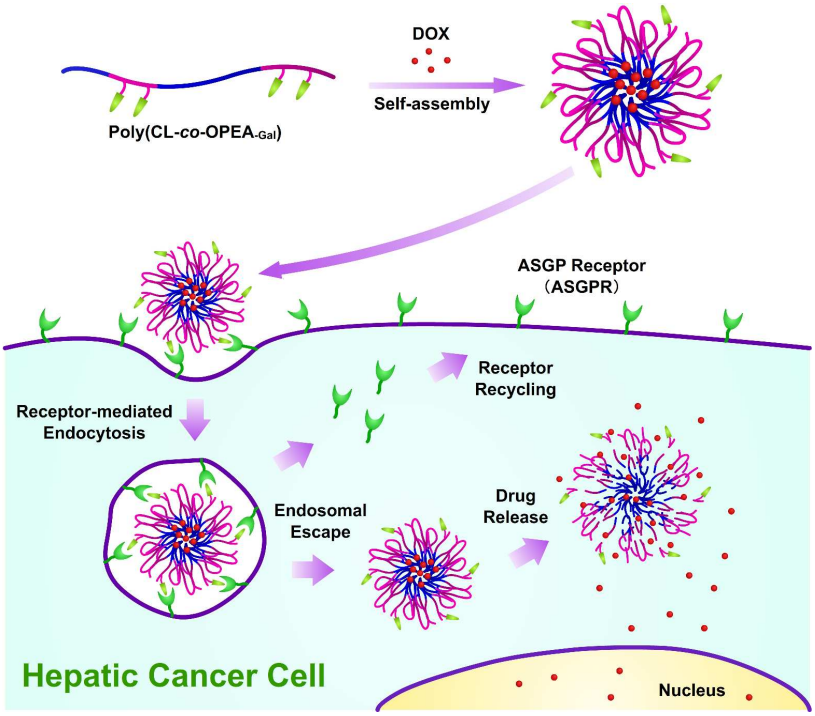

A novel biocompatible and biodegradable poly(ε-caprolactone-*co*-phosphoester) random copolymer conjugated with galactosamine has been synthesized and used for enhanced hepatoma-targeting delivery of Doxorubicin.

Cite this: DOI: 10.1039/c0xx00000x

www.rsc.org/xxxxxx

ARTICLE TYPE

Galactosylated Biodegradable Poly(ε-caprolactone-*co*-phosphoester) Random Copolymer Nanoparticles for Potent Hepatoma-Targeting Delivery of Doxorubicin

Yunfeng Tao[a], Jinlin He[a], Mingzu Zhang[a], Ying Hao[a], Jian Liu[b] and Peihong Ni[a,*]

Received (in XXX, XXX) Xth XXXXXXXXX 20XX, Accepted Xth XXXXXXXXX 20XX
DOI: 10.1039/b000000x

A novel galactosamine (Gal)-mediated drug delivery carrier, Gal-conjugated biodegradable poly(ε-caprolactone-*co*-phosphoester) random copolymer [poly(CL-*co*-OPEA$_{-Gal}$)], was developed for enhanced hepatoma-targeting delivery of anti-cancer drug doxorubicin (DOX). The functionalized copolymers were synthesized via a combination of ring-opening polymerization (ROP), photoinduced thiol-ene reaction and amidation reaction. The chemical composition and structures, as well as the the molecular weights and molecular weight distributions of these copolymers were characterized by ^{1}H NMR, ^{31}P NMR and GPC analyses. Morphological study indicated that all the poly(CL-*co*-OPEA$_{-Gal}$) nanoparticles (Gal-NP), DOX-loaded nanoparticles (DOX/Gal-NP), pristine polymeric nanoparticles without Gal modification (NP) and DOX-loaded nanoparticles without Gal modification (DOX/NP) displayed spherical shape with averaged diameters below 200 nm. The *in vitro* drug release behavior of DOX/Gal-NP was featured with a pH-dependent manner due to the degradable components of the random copolymer sensitive to the environmental stimuli. Cellular uptake studies demonstrated that DOX/Gal-NP can be internalized into HepG2 cells more efficiently compared with HeLa cells owing to specific ligand-receptor interactions between Gal and asialoglycoprotein receptors (ASGPR) on the surface of HepG2 cells. *In vitro* cytotoxicity tested by MTT assay indicated that these random copolymers performed favorable biocompatibility. And DOX/Gal-NP exhibited a higher antitumor efficacy than DOX/NP against HepG2 cells. These results show that these biodegradable Gal-decorated poly(CL-*co*-OPEA$_{-Gal}$) nanoparticles are highly promising for targeted delivery of water-insoluble anti-cancer drugs for hepatocellular carcinoma.

Introduction

Nowadays, cancers remain the most disastrous diseases worldwide, with more than ten million new cases every year. As one of the main therapeutic approaches, chemotherapy can destroy tumors and inhibit cancer progress. However, it is usually restricted by the severe cytotoxicity of anticancer drugs to normal tissues and cells.[1,2] To this end, researchers have paid much attention to various drug formulations (nanoparticle, micelle, emulsion, etc.) to reduce the side effects and improve the therapeutic effectiveness of anticancer drugs.[3] Among them, polymeric micelles have become one of the most promising carriers especially for poorly water-soluble anticancer drugs, such as the clinically widely used paclitaxel (PTX) and doxorubicin (DOX).[4-7] This method can not only enhance the water solubility of drugs and prolong their circulation time, but also greatly improve drug bioavailability via passive targeting by the enhanced permeability and retention (EPR) effect,[7] or active targeting by conjugation of various molecules including folate,[8-10] peptides,[11-14] carbohydrates[15,16] and antibodies.[17,18]

In particular, polymeric micelles, which are composed of biocompatible and biodegradable amphiphilic copolymers, have been one of the most promising carriers because of their attractive properties including low immunogenicity, low toxicity, and good biodegradability, etc.[16,19,20] As representative candidates, aliphatic biodegradable polyesters such as polylactide (PLA), poly(ε-caprolactone) (PCL), and poly(lactide-*co*-glycolide) (PLGA) have been widely used in controlled drug delivery.[21,22] They can be degraded by hydrolytic or enzymatic degradation under physiological conditions, and the properties can be easily tuned through rational molecular design. Notably, a number of micellar anticancer drug formulations have already progressed to the different stages of the clinical trials.[23] For example, Genexol®-PM consisting of Paclitaxel and methoxy polyethylene glycol-*block*-poly(D, L-lactide) has shown satisfactory therapeutic efficacy during Phase I study,[24,25] and the Phase II study is still under investigation.

Meanwhile, we have noticed that most of the frequently used hydrophilic polymers in constructing drug carriers are poly(ethylene glycol), poly(*N*-isopropyl acrylamide) or poly(2-hydroxypropyl methacrylate). Although these polymers show favorable biocompatibility, a major concern arises from their poor biodegradability. In the past years, polyphosphoesters (PPEs) have received growing attentions in biomedical applications due

to their adjustable hydrophilicity, excellent biocompatibility and biodegradability, as well as facile functionalization.[26-31] Moreover, it has been proved that Phosphodiesterase I existed in cytosome or subcellular regions of human cells can accelerate degradation of polyphosphoesters. Therefore, many research groups have made great contributions to this field, and a variety of formulations for anticancer drugs delivery have been constructed and examined, such as micelles,[30,32,33] polymeric prodrugs,[10,34-36] hydrogels or nanogels.[37-41] In our previous work, we have prepared a biodegradable diblock copolymer, poly(ε-caprolactone)-*block*-poly[2-(2-oxo-1, 3, 2-dioxaphospholoyloxy) ethyl acrylate] (PCL-*b*-POPEA), in which the acryloyl groups in the pendants of POPEA moiety could covalently conjugated with various functional mercaptan agents through Michael-type addition to form new pendant groups such as hydroxyl, carboxyl, amine, and amino acid, respectively.[33]

In this paper, we aim to develop an easier synthesis route and introduce galactosamine for constructing a liver-targeting antitumor drug carrier. Considering the steric effect of cyclic galactosamine (Gal) and avoiding the cross-linking tendency due to the close acryloyl groups in POPEA segments, the random copolymers poly(CL-*co*-OPEA) were first prepared via ROP reaction in one-pot process. And then liver-targeting galactosamine was conjugated to the hydrophilic polyphosphoester segments, yielding the targeting amphiphilic copolyesters poly(CL-*co*-OPEA$_{-Gal}$). This galactosylated copolymer could self-assemble into stable micelles in aqueous solution with hydrophobic PCL as the core, hydrophilic polyphosphoester as the corona, and Gal moiety on the micellar surface. These micelles could be used as potential antitumor drug carriers for hepatoma-targeting drug delivery and increased hepatic internalization to improve therapeutic efficiency.

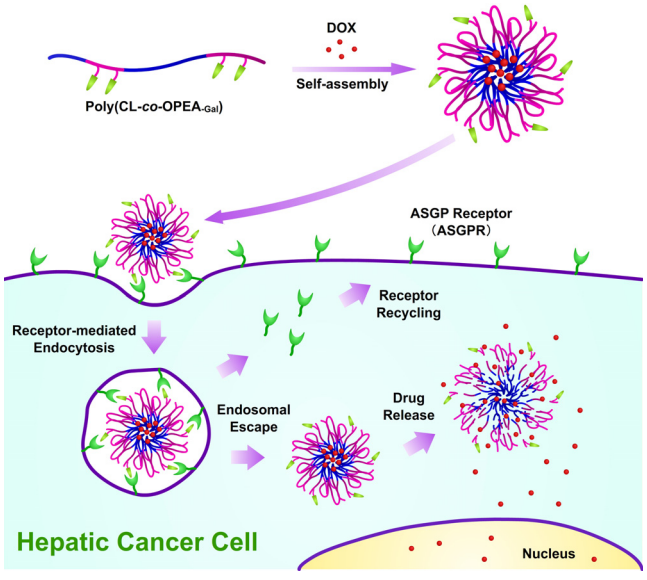

Scheme 1 Schematic illustration of the preparation of hepatoma-targeting DOX-loaded poly(CL-*co*-OPEA$_{-Gal}$) nanoparticles (designated as DOX/Gal-NP) and the receptor-mediated intracellular drug release.

Scheme 1 shows a representive process of the formation of hepatoma-targeting DOX-loaded poly(CL-*co*-OPEA$_{-Gal}$) nanoparticles and the receptor-mediated intracellular drug release. Since there are large numbers of asialoglycoprotein receptors (ASGPR) that recognize galactose and galactosamine residues on the surface of hepatocytes, it is anticipated that these fully biodegradable polymeric nanoparticles bearing Gal moieties would allow efficient targeting and uptake by ASGPR over-expressing hepatoma cells via a receptor-mediated endocytosis process.[16,42-45]

Experimental

Materials

2-(2-oxo-1, 3, 2-dioxaphospholoyloxy) ethyl acrylate (OPEA) was synthesized just before use as we described previously.[33] ε-Caprolactone (ε-CL, 99%, Sigma-Aldrich) was dried over calcium hydride for one day at room temperature and distilled under reduced pressure before use. Stannous octoate [Sn(Oct)$_2$] (99%, Sigma-Aldrich) was distilled before use. Ethylene glycol, benzene, dichloromethane, benzyl alcohol (BzOH), toluene, triethylamine (TEA) and dimethyl sulfoxide (DMSO) were all AR grade and purchased from Sinopharm Chemical Reagent Co. and distilled before use. Tetrahydrofuran (THF, AR, Sinopharm) was initially dried over potassium hydroxide for at least two days and then refluxed over sodium wire with benzophenone as an indicator until the color turned purple. 2-Hydroxyethyl acrylate (HEA, 99%, TCI), 3-mercaptoacetic acid (99%, Acros), 2, 2-dimethoxy-2-phenylacetophenone (DMPA, 98%, TCI), D-(+)-galactosamine hydrochloride (98%, Shanghai Yuanju Biotechnology Co.), 1-(3-dimethylaminopropyl)-3-ethylcarbodiimide hydrochloride (EDC, 99%, Shanghai Medpep Co.), *N*-hydroxysuccinimide (NHS, 98%, Sigma-Aldrich), pyrene (99%, Sigma-Aldrich), doxorubicin hydrochloride (DOX, 99%, Beijing Zhongshuo Pharmaceutical Technology Development Co.), bisbenzimide H 33342 trihydrochloride (H 33342, 98%, Sigma-Aldrich), thiazolyl blue tetrazolium bromide (MTT, 98%, Sigma-Aldrich) and other chemicals were used as received. All cell culture related reagents were purchased from Invitrogen.

Synthesis of random copolymer poly(CL-*co*-OPEA)

Poly(CL-*co*-OPEA) was synthesized via ROP reaction of ε-CL and OPEA using BzOH as the initiator and Sn(Oct)$_2$ as the catalyst. Briefly, one 50 mL of Schlenk flask with a magnetic stirring bar was dried at 120 °C for 12 h and cooled by an exhausting-refilling with argon process for three times. BzOH (0.10 g, 0.93 mmol) and 10 mL of anhydrous toluene were added into the flask by syringe, ε-CL (4.51 g, 39.43 mmol), OPEA (2.24 g, 10.08 mmol) and Sn(Oct)$_2$ (0.01 g, 0.03 mmol) were then consecutively added under the protection of argon. The reaction was carried out at 80 °C for 24 h. Afterward, the mixture was concentrated under reduced pressure and precipitated in ethyl ether/methanol (volume ratio v/v, 10:1). The random copolymer was obtained after drying under vacuum at 25 °C for 24 h (5.27 g, Yield: 77.3%).

Synthesis of carboxyl group functionalized copolymer poly(CL-*co*-OPEA$_{-COOH}$)

In order to conjugate galactosamine onto the pendants of polyphosphoester units, the acryloly groups of poly(CL-*co*-OPEA) were first converted into carboxyl groups via photoinduced thiol-ene reaction. In an open vial, poly(CL-*co*-OPEA) (100 mg, 0.023 mmol, 0.138 mmol acryloyl group), DMPA (1.7 mg, 6.6 μmol) and 3-mercaptopropionic acid (21.7 mg, 0.22 mmol) were dissolved in 3 mL of $CHCl_3$. After irradiation with UV 365 nm for 30 min, the mixture was precipitated into 100 mL of cold diethyl ether. The precipitate was collected, redissolved in DMF, and dialyzed against Milli-Q water for 4 days, and water was exchanged at appropriate intervals during the dialyzing process. The product poly(CL-*co*-OPEA$_{-COOH}$) was finally obtained after lyophilization (68.2 mg, Yield: 60.1%).

Synthesis of galactosamine-conjuagted random copolymer poly(CL-*co*-OPEA$_{-Gal}$)

Galactosylated poly(CL-*co*-OPEA) was prepared via amidation reaction between carboxyl groups of poly(CL-*co*-OPEA$_{-COOH}$) and the amino groups of galactosamine. Poly(CL-*co*-OPEA$_{-COOH}$) (49.2 mg, 0.011 mmol) was firstly activated at 25 °C in the presence of EDC (14.4 mg, 0.075 mmol) and NHS (4.9 mg, 0.043 mmol) in 10 mL of anhydrous DMSO for 12 h. Subsequently, D-(+)-galactosamine hydrochloride (9.5 mg, 0.044 mmol) and TEA (32.2 mg, 0.31 mmol) in 5 mL of anhydrous DMSO was added dropwise to the reaction and further stirred at 25 °C for 24 h. The mixture was dialyzed against Milli-Q water for 4 days with fresh water exchanged at appropriate intervals, and the product poly(CL-*co*-OPEA$_{-Gel}$) was obtained after lyophilization as white solid (37.9 mg, Yield: 64.6%).

Characterizations

All nuclear magnetic resonance (NMR) spectra were recorded on an INOVA-400 NMR spectrometer at room temperature with DMSO-d_6 or $CDCl_3$ as the solvent. The molecular weights and molecular weight distributions (PDI) of polymers were measured by a Waters 1515 gel permeation chromatography (GPC) instrument equipped with a set of MZ-Gel SDplus columns (500 Å, 10E3 Å, 10E4 Å) following a Waters 2414 refractive-index detector. The measurements were performed using DMF containing 0.05 mol L^{-1} LiBr as the eluent with a flow rate of 0.8 mL min^{-1} at 35 °C and a series of narrowly-distributed polystyrene standards were used as the calibration.

To estimate the critical aggregation concentration (CAC) values of the random copolymers, pyrene was used as the fluorescence probe. Typically, 50 μL of pyrene solutions in acetone (0.12 mg mL^{-1}) were added into a series of ampoules, and acetone was then evaporated under reduced pressure. Afterward, 5 mL of copolymer solutions in Milli-Q water with different concentrations were respectively added into the ampoules, and the concentration of pyrene was kept at 6×10^{-6} mol L^{-1}. The mixtures were sonicated for 30 min and further stirred for 24 h at room temperature before measurement. The fluorescence spectra were recorded by a FLS920 spectrofluorometer (Edinburgh Co., UK). Excitation was carried out at 335 nm, and emission spectra were recorded ranging from 350 nm to 500 nm. Both the slit width for excitation and emission were set at 1 nm. The intensity ratio (I_3/I_1) of the third band (383 nm, I_3) to the first band (372 nm, I_1) from the emission spectra was analyzed as a function of the polymer concentration. The CAC value was determined from the crossover point in the low concentration range.

The morphologies of the self-assembled nanoparticles were observed on a transmission electron microscopy (TEM) instrument (TECNAI G^2 20, FEI Co.) operated at 200 kV. 5 μL of the polymer solution was dropped onto a carbon-coated copper grid (400 meshes), which was allowed to evaporate at ambient temperature for 2 days before measurement.

The size and size distribution of the self-assembled nanoparticles in Milli-Q water were measured by a dynamic light scattering instrument (Zetasizer Nano ZS, Malvern) equipped with a 633 nm He-Ne laser using backscattering detection. The measurements were carried out at 25 °C with a scattering angle of 90 °.

Preparation of poly(CL-*co*-OPEA) and poly(CL-*co*-OPEA$_{-Gal}$) nanoparticles

The nanoparticles self-assembled from random copolymers were prepared by a dialysis method. Briefly, 25 mg of polymer was first dissolved in 5 mL of DMF, followed by dropwise adding 10 mL of Milli-Q water at the rate of 2 mL h^{-1} under moderate stirring. Subsequently, the mixture was kept stirring for an additional 4 h and dialyzed (MWCO 3500) against Milli-Q water for 48 h.

***In vitro* drug loading and release**

DOX-loaded polymeric nanoparticles were prepared as follows: 25 mg of random copolymer [poly(CL-*co*-OPEA) or poly(CL-*co*-OPEA-$_{Gal}$)] was dissolved in 5 mL of DMF, followed by adding 5 mg of DOX·HCl and 2 μL of TEA. The mixture was then stirred at room temperature in dark for 4 h, and 6 mL of Milli-Q water was added dropwise at the rate of 2.0 mL h^{-1}. Subsequently, the solution was stirred for another 4 h and dialyzed (MWCO 3500) against Milli-Q water for 24 h. The solution was finally diluted to the concentration of 1 mg mL^{-1}. For the determination of drug loading content, 5 mL of the DOX-loaded solution was lyophilized, redissolved in 5 mL of DMF and stirred for 48 h. The solution was measured by fluorescence spectroscopy with excitation at 480 nm and emission at 590 nm, and the concentration of DOX was calculated according to a calibration curve. The drug loading content (DLC) and drug loading efficiency (DLE) were calculated according to the following equations:

$$\text{DLC (\%)} = \frac{\text{weight of DOX loaded in nanoparticles}}{\text{weight of polymer}} \times 100 \quad (1)$$

$$\text{DLE (\%)} = \frac{\text{weight of DOX loaded in nanoparticles}}{\text{weight of DOX in feed}} \times 100 \quad (2)$$

The DOX release experiments were carried out in two kinds of phosphate buffer (PB, 10 mM) solutions (pH 7.4 and pH 5.0). In each experiment, 5 mL of DOX-loaded nanoparticle solution was transferred into a dialysis bag (MWCO 3500) and immersed into a tube containing 20 mL of buffer solution in a shaking water bath at 37 °C. At predetermined time intervals, 5 mL of the release medium was withdrawn for fluorescence spectroscopy analysis and replaced with 5 mL of fresh buffer solution to keep a

constant volume. The fluorescence intensities were measured with excitation at 480 nm and emission at 590 nm to determine the content of released DOX. All the release experiments were conducted in triplicate and the reported results are the average values with standard deviations.

In vitro antitumor study

Cell culture

HepG2 cells and HeLa cells were obtained from American Type Culture Collection (ATCC), and were separately cultured in DMEM containing 10% heat-inactivated fetal bovine serum (FBS), and 1% penicillin/streptomycin solution. The culture media were replaced every three days. The cells were cultured at 37 °C in an atmosphere containing 5% CO_2 and used in their growth state.

In vitro cytotoxicity

DOX-laoded polymeric nanoparticles formed from poly(CL-*co*-OPEA) or poly(CL-*co*-OPEA$_{\text{-Gal}}$) with DOX were desigated as DOX/NP or DOX/Gal-NP, respectively. Their relative cytotoxicity toward HepG2 cells and HeLa cells were evaluated by the MTT assay, using free DOX and blank poly(CL-*co*-OPEA$_{\text{-Gal}}$) nanoparticles as the controls. Cells were seeded in 96-well plates at a density of 1×10^4 cells per well in 100 μL of DMEM medium, and incubated at 37 °C in 5% CO_2 atmosphere for 12 h, followed by adding DOX-loaded nanoparticles, blank nanoparticles and free DOX solutions at different concentrations. After 48 h incubation, 20 μL of MTT stock solution (5 mg mL^{-1} in PBS) was added to each well. After incubation for an additional 4 h, DMEM medium was removed and 150 μL of DMSO was added to each well. Finally, the absorbance at 570 nm of each well was measured by a microplate reader (Bio-Rad 680) to obtain the optical density (OD) value. The OD values were normalized to wells in which cells were not treated with any samples. Data are presented as the average values with standard deviations.

Cellular uptake

The cellular uptake experiments were respectively performed using live cell imaging system (CELL'R, Olympus, Japan) and flow cytometry (Cytomics FC500, Beckman Coulter, American). The real-time observation of the uptake of DOX/NP or DOX/Gal-NP by HepG2 cells or HeLa cells was achieved using live cell imaging system. HepG2 cells and HeLa cells were seeded onto 35-mm glass bottom cell culture dishes at a density of 2×10^4 cells cm^{-2} for 12 h prior to the experiment. Afterward, culture medium was removed, cells were carefully washed with PBS, followed by staining with H 33342 for 15 min and washing with PBS again. Finally, 1 mL of fresh culture medium containing DOX/NP or DOX/Gal-NP (final concentration of DOX: 0.1 mg L^{-1}) was added. The culture dish was mounted in the incubation system of the live cell imaging system at 37 °C under 5% CO_2.

For flow cytometry analysis, HepG2 cells were seeded onto 35-mm cell culture dishes at a density of 2×10^4 cells cm^{-2} and allowed to adhere for 12 h. Subsequently, the culture medium was replaced by 1 mL of fresh medium containing DOX/NP or DOX/Gal-NP (final concentration of DOX: 0.1 mg L^{-1}). After incubation at 37 °C for different time, the culture medium was removed, cells were then washed with PBS for three times and digested with trypsin. After that, 2 mL of culture medium was added to each culture dish, and the solutions were centrifuged for 3 min at 1000 rpm. After the removal of the supernatants, the cells were resuspended in 0.5 mL of PBS. The fluorescence histograms of DOX in cells was recorded using flow cytometry.

Results and discussion

Synthesis and characterization of poly(CL-*co*-OPEA$_{\text{-Gal}}$) copolymers

As shown in Scheme 2, poly(CL-*co*-OPEA$_{\text{Gal}}$) random copolymers were prepared in three steps. Poly(CL-*co*-OPEA) copolymers were firstly synthesized via a random ROP reaction of ε-CL and OPEA using BzOH as the initiator and $Sn(Oct)_2$ as the catalyst; And then, galactosamine (Gal) was covalently conjugated with the polyphosphoester units via a combination of photoinduced thiol-ene reaction and amidation reaction.

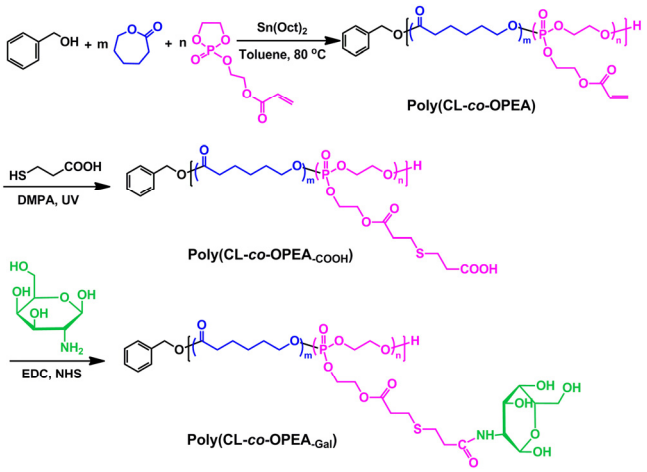

Scheme 2 Synthesis routes of galactosamine-conjugated random copolymer poly(CL-*co*-OPEA$_{\text{-Gal}}$).

Fig. 1 shows the ^{1}H NMR spectra of poly(CL_{62}-*co*-$OPEA_{10}$), poly[CL_{62}-*co*-$(OPEA_{\text{-COOH}})_{10}$] and poly[$CL_{62}$-*co*-$(OPEA_{\text{-Gal}})_{10}$], respectively. One can find all the signals assigned to the protons of the polymers. Comparaed with the ^{1}H NMR spectrum of poly(CL_{62}-*co*-$OPEA_{10}$) in Fig. 1(A), the proton signals ascribed to acryloyl groups (-CO-C***H***=C***H***$_2$) at δ 5.95 ppm, δ 6.18 ppm and δ 6.35 ppm have completely disappeared in Fig. 1(B) after thiol-ene reaction, and the appearance of new signals corresponding to the methylene protons (-SC***H***$_2$C***H***$_2$COOH) at δ 2.7 ppm and carboxyl proton (-SCH_2CH_2COO***H***) at δ 12.2 ppm. These results confirm the successful synthesis of poly[CL_{62}-*co*-$(OPEA_{\text{-COOH}})_{10}$]. Furthermore, the conjugation between carboxyl groups and amino groups to form poly[CL_{62}-*co*-$(OPEA_{\text{-Gal}})_{10}$] were proved by the disappearance of carboxyl group and newly appeared proton signals corresponding to Gal segment, as shown in Fig. 1(C). ^{31}P NMR analysis was also further carried out to confirm the chemical structure, and the comparison of ^{31}P NMR spectra of OPEA monomer and poly(CL_{62}-*co*-$OPEA_{10}$) is depicted in Fig. 2, in which the spectrum of OPEA monomer has a strong resonance at δ 18.22 ppm in Fig. 2(A), whereas for poly(CL_{62}-*co*-$OPEA_{10}$) copolymer shown in Fig. 2(B) the strong resonance shifts to δ -1.11 ppm, assigning to the phosphorus atoms in polyphosphoester backbone.

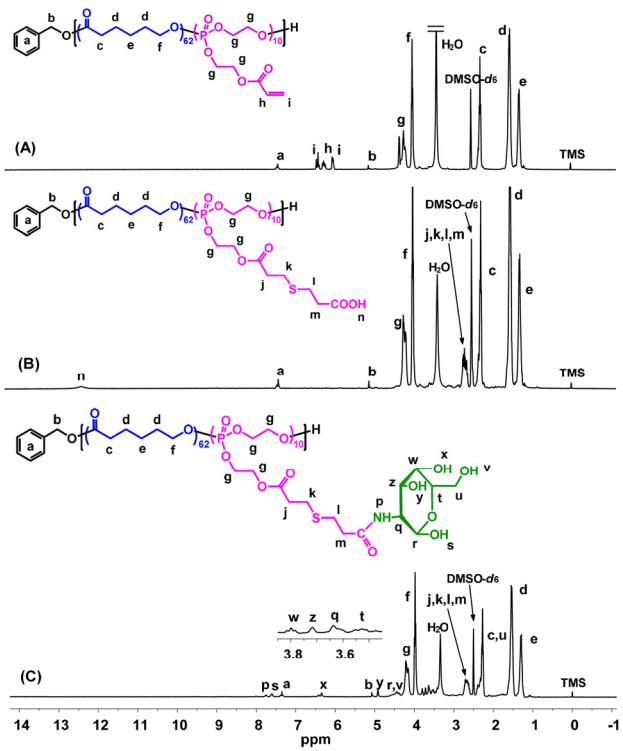

Fig. 1 ^{1}H NMR spectra of (A) poly(CL_{62}-*co*-$OPEA_{10}$), (B) poly[CL_{62}-*co*-($OPEA_{-COOH}$)$_{10}$] and (C) poly[CL_{62}-*co*-($OPEA_{-Gal}$)$_{10}$] in DMSO-d_6.

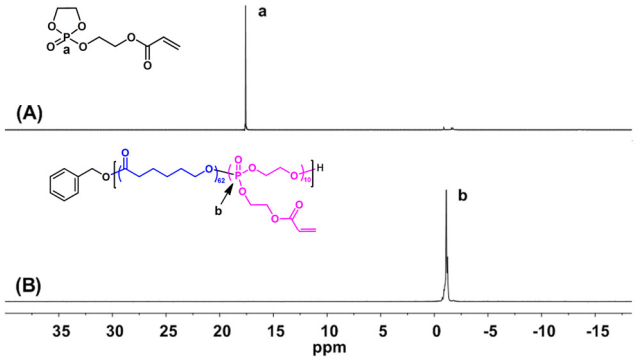

Fig. 2 ^{31}P NMR spectra of (A) OPEA monomer and (B) poly(CL_{62}-*co*-$OPEA_{10}$) in $CDCl_3$.

Based on the ^{1}H NMR spectrum in Fig. 1(A), the degrees of polymerization (m and n) of PCL and POPEA in poly(CL_m-*co*-$OPEA_n$) were respectively calculated by eqn (3) and (4), where A_b is the integral area of the protons of methylene group (signal *b*, δ 5.06 ppm) in benzyl segment, A_f is the integral area of the protons of methylene group adjacent to oxygen (signal *f*, δ 3.96 ppm) in PCL chain, and A_g represents the integral area of methylene protons (signal *g*, δ 4.20 ppm) in POPEA chain.

$$m = \frac{A_f}{A_b} \qquad (3)$$

$$n = \frac{A_g}{4A_b} \qquad (4)$$

Therefore, the molecular weights of poly(CL_m-*co*-$OPEA_n$) could be obtained according to eqn (5), where 114.1, 222.1 and 108.1 are the molecular weights of one repeating unit of PCL, one repeating unit of POPEA and benzyl alcohol, respectively.

$$\bar{M}_{n,NMR} = 114.1 \times m + 222.1 \times n + 108.1 \qquad (5)$$

Table 1 lists the characterization data of a series of poly(CL_m-*co*-$OPEA_n$) random copolymers, and the molecular weights can be controlled by simply changing the molar ratios of monomers and the initiator. The narrow PDI values indicated the well control of molecular weight distributions.

Table 1 Characterization data of the compositions, number-average molecular weights and molecular weight distributions (PDIs) of poly(CL_m-*co*-$OPEA_n$) copolymers.

Samples	$\bar{M}_{n,NMR}$ [a] (g mol^{-1})	$\bar{M}_{n,GPC}$ [b] (g mol^{-1})	PDI [b]
poly(CL_{23}-*co*-$OPEA_8$)	4510	8960	1.16
poly(CL_{87}-*co*-$OPEA_5$)	11150	12770	1.32
poly(CL_{64}-*co*-$OPEA_9$)	9410	11830	1.28
poly(CL_{26}-*co*-$OPEA_6$)	4410	10030	1.18
poly(CL_{35}-*co*-$OPEA_{16}$)	7660	8360	1.19
poly(CL_{25}-*co*-$OPEA_5$)	4070	6580	1.20
poly(CL_{62}-*co*-$OPEA_{10}$)	9400	10780	1.34

[a] Calculated by eqn (5) based on ^{1}H NMR analysis. [b] Measured by GPC with DMF as the eluent and polystyrene as standards.

Preparation and characterization of polymeric nanoparticles

In aqueous solution, the amphiphilic copolymers poly(CL-*co*-OPEA) could self-assemble into micelles with hydrophobic PCL segments as the core and hydrophilic polyphosphoester parts as the shell. The water-insoluble drugs such as DOX could be encapsulated into the nanoparticles through hydrophobic interactions. Herein, the self-assembly behaviors of four kinds of nanoparticles were investigated. The initially synthesized poly(CL_{26}-*co*-$OPEA_6$) without or with DOX loading were abbreviated as NP and DOX/NP, respectively, while the galactosylated copolymers poly[CL_{26}-*co*-($OPEA_{-Gal}$)$_6$] without or with DOX loading were simplified as Gal-NP and DOX/Gal-NP, respectively. The critical aggregation concentration (CAC) values of copolymers were first measured by fluorescence probe technique using pyrene as the probe. A series of copolymer solutions with different concentrations were prepared and the ratios of the third vibronic peaks to the first one (I_3/I_1) in pyrene fluorescence spectrum were recorded. The I_3/I_1 ratios were plotted as a function of the polymer concentrations as shown in Fig. 3, from which the CAC values of poly(CL_{26}-*co*-$OPEA_6$) and poly[CL_{26}-*co*-($OPEA_{-Gal}$)$_6$] are determined to be 0.46 mg L^{-1} and 4.38 mg L^{-1}, respectively. The conjugation of galactosamine with hydroxyl groups enhanced the hydrophilicity and resulted in the obvious increase of CAC value.

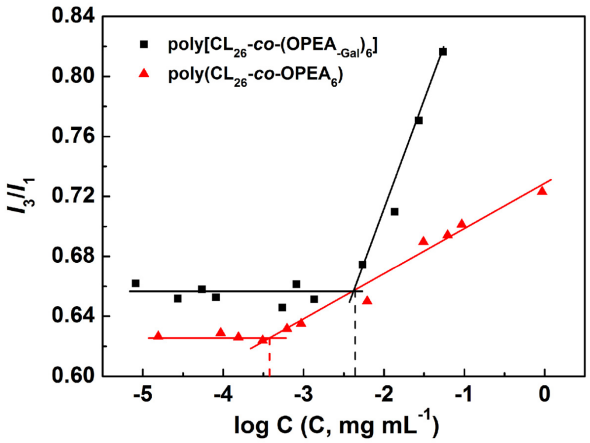

Fig. 3 Intensity ratios (I_3/I_1) in pyrene fluorescence emission spectrum as a function of logarithm concentration of poly(CL_{26}-*co*-$OPEA_6$) and poly[CL_{26}-*co*-$(OPEA_{-Gal})_6$] in aqueous solution.

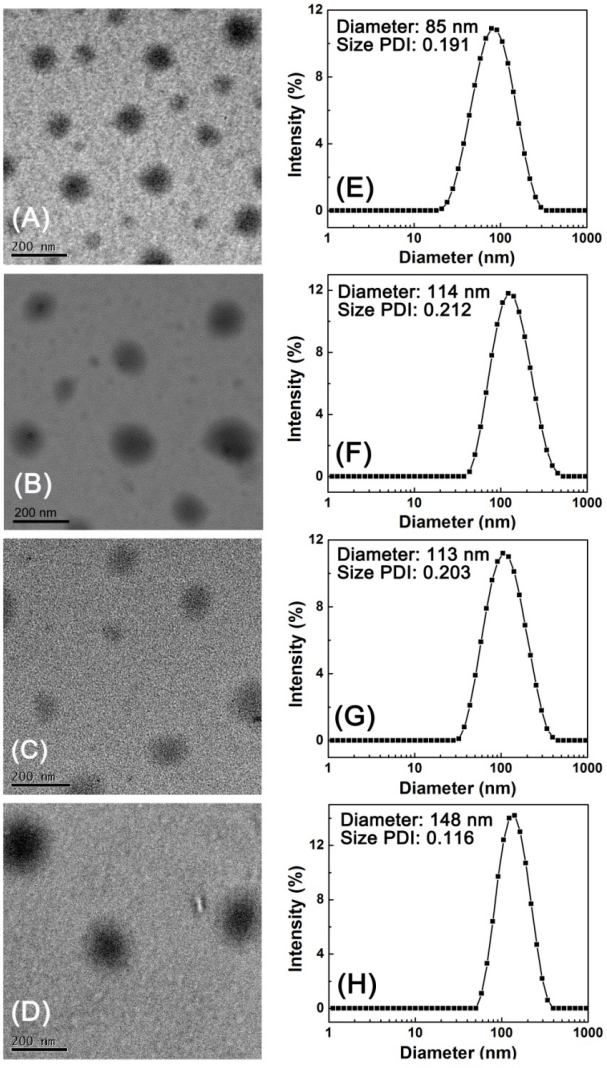

Fig. 4 TEM images of nanoparticles formed from (A) poly(CL_{26}-*co*-$OPEA_6$), (B) DOX-loaded poly(CL_{26}-*co*-$OPEA_6$), (C) poly[CL_{26}-*co*-$(OPEA_{-Gal})_6$] and (D) DOX-loaded poly[CL_{26}-*co*-$(OPEA_{-Gal})_6$]; their particle size distribution curves are corresponding to (E), (F), (G) and (H), respectively.

Particle size and particle size distribution are important parameters of nanocarriers for drug delivery. It is widely reported that drug-loaded nanoparticles with appropriate sizes less than 200 nm can extravasate into the tumor tissues via the leaky vessels by EPR effect, and then release drugs into the vicinity of the tumor cells.[46,47] The micellization of amphiphilic random copolymers was further verified by TEM and DLS analyses. Fig. 4(A) and (C) show the typical TEM images of NP and Gal-NP in water, respectively, from which one can find that all these nanoparticles are spherical with the average diameters of around 100 nm. The corresponding particle size distribution curves were measured by DLS as shown in Fig. 4(E) and (G), which show the average diameters of 85 nm and 113 nm for NP and Gal-NP nanoparticles respectively. Similarly, the properties of DOX-loaded nanoparticles DOX/NP and DOX/Gal-NP were characterized by TEM and DLS. Comparing Fig. 4(A) and (B), the average diameter of DOX/NP is larger than that of NP. The same result can be observed by comparing Fig. 4(C) and (D). Furthermore, DLS results shown in Fig. 4(F) and (H) indicate that the average diameters of DOX/NP and DOX/Gal-NP increased to 114 and 148 nm compared with corresponding blank nanoparticles 85 and 113 nm in Fig. 4(E) and (G), respectively. The increase of particle size may be ascibed to the increasing volume of hydrophobic core after DOX loading process.

In vitro cytotoxicity

Biocompatibility is one of the significant factors for the application of polymeric materials in drug delivery. Herein, the cytotoxicity of poly(CL_{26}-*co*-$OPEA_6$) and poly[CL_{26}-*co*-$(OPEA_{-Gal})_6$] against HepG2 cells and HeLa cells were studied by the MTT assays. Fig. 5 shows the cell viabilities of HepG2 cells and HeLa cells after 48 h incubation with two kinds of copolymers with and without Gal moiety at different concentrations. Both copolymers show low toxicity against either HepG2 cells or HeLa cells at various concentrations, and the cell viabilities are still higher than 80% even at the concentration up to 200 mg L^{-1}. The results suggest excellent biocompatibility of these random copolymers.

In vitro DOX loading and release

The poly[CL_{26}-*co*-$(OPEA_{-Gal})_6$] nanoparticles with favorable biocompatibility and appropriate sizes were examined for drug delivery. The anticancer drug DOX was encapsulated into the hydrophobic core using a dialysis method. The drug loading content (DLC) and drug loading efficiency (DLE) calculated from fluorescence measurement were 2.8% and 14.1%, respectively. DOX-loaded poly(CL_{26}-*co*-$OPEA_6$) nanoparticles, of which the DLC and DLE were respectively determined to be 3.6% and 18.2%, were prepared as the control trials.

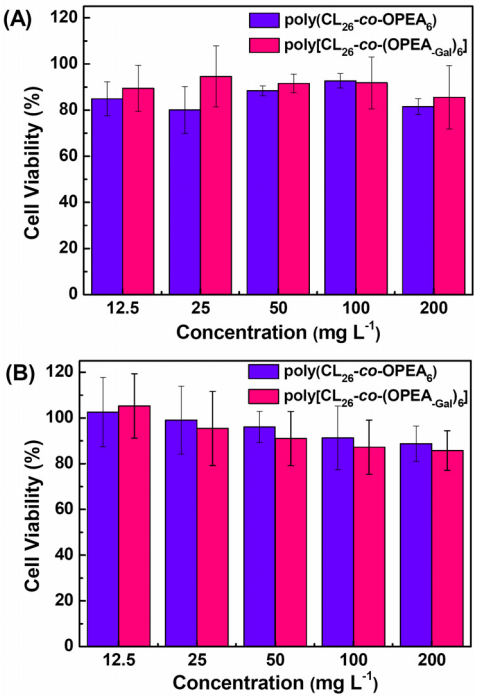

Fig. 5 Cell viability of (A) HepG2 cells and (B) HeLa cells, treated with poly(CL_{26}-*co*-$OPEA_6$) and poly[CL_{26}-*co*-$(OPEA_{-Gal})_6$] with different concentrations for 48 h incubation.

The *in vitro* cumulative release of DOX was investigated in two kinds of phosphate buffer solutions (pH 7.4 and pH 5.0). According to Fig. 6, it can be observed that the cumulative DOX release was only about 20 % at pH 7.4 over 80 h, implying that the nanoparticles were relatively stable under neutral condition. And the DOX/Gal-NP and DOX/NP showed similar release behavior at the same pH condition. However, in a mildly acidic environment (pH 5.0), the release rate was significantly accelerated and the cumulative DOX release inreased to about 80% over the same release time. This highly pH-responsive release behavior of nanoparticles could be ascribed to the acid-accelerated hydrolytic degradation of polyphosphoester,[36,48] resulting in the disruption of nanoparticles under acidic condition. Therefore, it is anticipated that these DOX-loaded poly(CL-*co*-$OPEA_{-Gal}$) nanoparticles can realize pH-triggered release under acidic condition in tumor cell environment.[49]

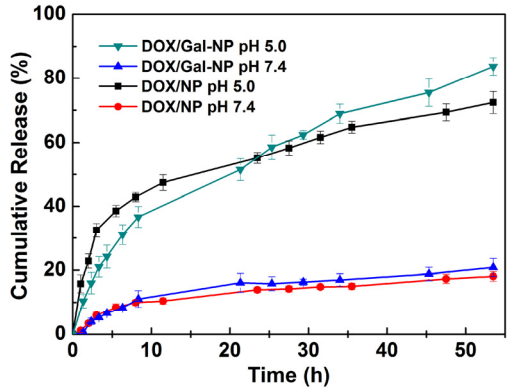

Fig. 6 *In vitro* release profile of DOX from DOX-loaded poly[CL_{26}-*co*-$(OPEA_{-Gal})_6$] nanoparticles (DOX/Gal-NP) and DOX-loaded poly(CL_{26}-*co*-$OPEA_6$) nanoparticles (DOX/NP) incubated in pH 5.0 buffer solution and 7.4 buffer solution at 37 °C.

Cellular uptake and intracellular DOX release of polymeric nanoparticles

It is well-documented that the asialoglycoprotein receptors (ASGPR) overexpressed on the surfaces of hepatocytes are able to recognize galactose and galactosamine (Gal), resulting in the enhanced internalization of Gal-conjugated nanocarriers and the receptor recycles back to the surface of cells.[2,44] To evaluate the extents of internalization of the prepared nanoparticles, HepG2 and HeLa cells were incubated with DOX/NP or DOX/Gal-NP for different time. HeLa cells, lack of ASGPR, was selected as a negative control cell line in the present study. The cellular uptake behaviors were real-time monitored using live cell imaging system. The cell nuclei were stained with H 33342 (blue). As shown in Fig. 7(A), DOX/Gal-NP starts to be internalized into HepG2 cells after 1 h incubation and red fluorescence intensity of DOX with a gradual increase can be observed with the increase of incubation time. After 12 h incubation, a significant portion of DOX/Gal-NP was internalized by HepG2 cells. In comparison, as shown in Fig. 7(B), the fluorescence of DOX in Hela cells is relatively weaker than Fig. 7(A) after 12 h incubation, indicating that less amount of DOX/Gal-NP was internalized by HeLa cells than that by HepG2 cells. In addition, the selective internalization of DOX/NP and DOX/Gal-NP by HepG2 cells was further investigated by flow cytometry analysis for quantitative determination of the cellular uptake of DOX. Fig. 8(A) evidently reveals that the relative geometrical mean fluorescence intensities (GMFI) of the internalized DOX/Gal-NP by HepG2 cell increased regularly with the incubation time. It is noteworthy that incubating DOX/NP without Gal moiety on the surface displayed much smaller GMFI than that of DOX/Gal-NP after equal incubation time, as illustrated in Fig. 8(B).Therefore, these results further confirm that Gal greatly improved the specific cell binding and cellular uptake of DOX-loaded nanoparticles by ASGPR-overexpressing HepG2 cells.

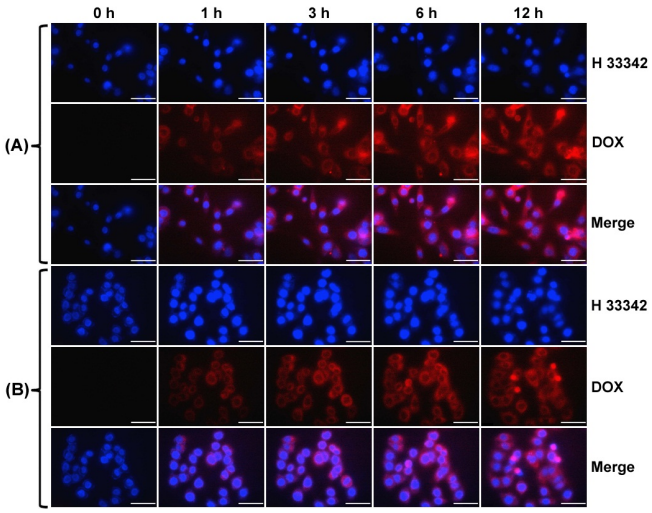

Fig. 7 Comparison on the fluorescence images of (A) HepG2 cells and (B) HeLa cells incubating with DOX/Gal-NP for different time. The dosage of DOX was 0.1 mg L^{-1}. For each panel, images from up to down show cell nuclei stained by H 33342 (blue), DOX fluorescence in cells (red) and overlays of two images. The scale bars correspond to 50 μm in all the images.

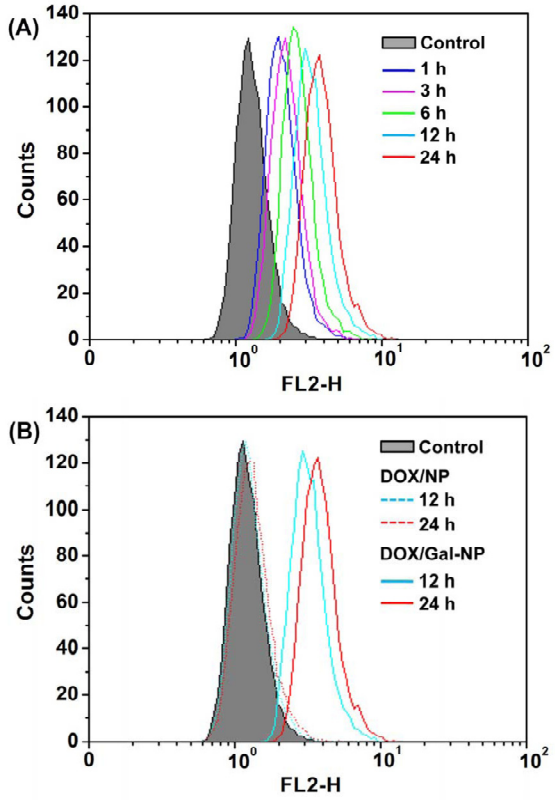

Fig. 8 Flow cytometry histogram profiles of HepG2 cells incubated with (A) DOX/Gal-NP for different time; and (B) DOX/NP and DOX/Gal-NP for 12 h and 24 h. The dosage of DOX was 0.1 mg L^{-1}.

As discussed above, such an enhanced cellular uptake and intracellular release of DOX from DOX/Gal-NP by HepG2 cells would lead to effective internalization and improved proliferation inhibition efficiency. Thus, the *in vitro* cytotoxicity of DOX-loaded micelles was determined by MTT assay. HepG2 cells were pretreated with the solutions of free DOX, DOX/NP and DOX/Gal-NP at different DOX concentrations ranging from 0.625 to 10 mg L^{-1} for 48 h, and then the cell viability was tested. As shown in Fig. 9(A), DOX/Gal-NP exhibits much higher cytotoxicity to HepG2 cells compared with DOX/NP. The IC_{50} (inhibitory concentration to produce 50% cell death) values of DOX/Gal-NP and DOX/NP were determined to be 1.17 and 10.01 mg DOX equiv L^{-1}, respectively, and the IC_{50} for free DOX (2.82 mg L^{-1}) was between them. The higher anti-tumor activity of DOX/Gal-NP indicated that DOX could be more efficiently delivered and released into the nuclei of HepG2 cells owing to Gal-mediated endocytosis. Moreover, HeLa cells were also treated with DOX/Gal-NP at the same DOX concentrations for 48 h incubation. The results shown in Fig. 9(B) indicate that DOX/Gal-NP shows a higher activity in inhibiting the growth of HepG2 cells than HeLa cells, supporting the enhancement by the specific interaction between DOX/Gal-NP and HepG2 cells.

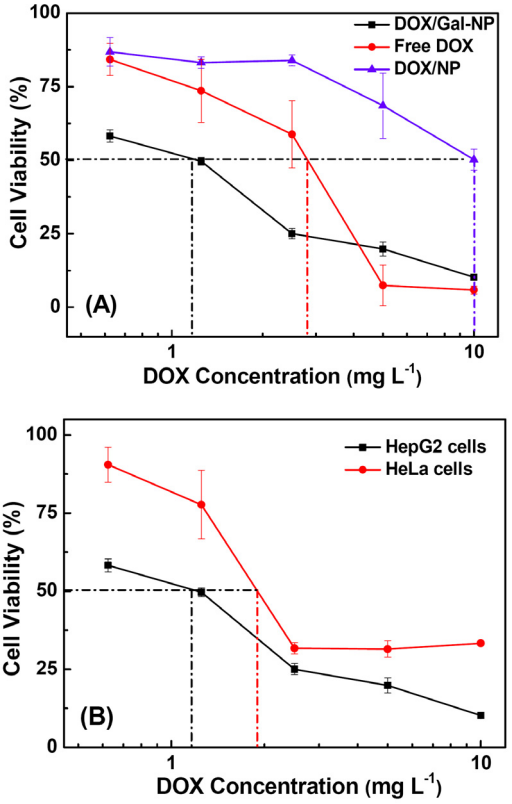

Fig. 9 Cell viability of (A) HepG2 cells treated with DOX/Gal-NP, free DOX and DOX/NP with different DOX dosages for 48 h incubation; and (B) HepG2 cells and HeLa cells treated with DOX/Gal-NP with different DOX dosages for 48 h incubation.

Conclusions

A novel actively targeting drug delivery carrier, galactosamine (Gal)-modified poly(ε-caprolactone-*co*-phosphoester) random copolymers [poly(CL-*co*-$OPEA_{-Gal}$)], were developed and evaluated in the present work. These copolymers could self-assemble into spherical micelles, and *in vitro* cytotoxicity and degradation results indicated their favorable biocompatibility and biodegradability. DOX-loaded polymeric nanoparticles (the average diameter of about 150 nm) carrying Gal moiety on the surfaces (DOX/Gal-NP) can be internalized into HepG2 cells via receptor-mediated endocytosis. They exhibited a pH-responsive drug release behavior. Moreover, DOX/Gal-NP showed a much higher activity in inhibiting the growth of asialoglycoprotein receptors (ASGPR) overexpressing HepG2 cells than that of HeLa cells. As expected, the results demonstrated that DOX/Gal-NP performed more efficiently in killing HepG2 cells than DOX/NP without Gal moiety. Consequently, the targeted nanoparticles formed from Poly(CL-*co*-$OPEA_{-Gal}$) can be employed as a promising anti-cancer drug carrier for liver cancer treatment.

Acknowledgements

The authors gratefully acknowledge financial support from the National Natural Science Foundation of China (21074078 and 21374066), Natural Science Foundation of Jiangsu Province for Rolling Support Project (BK2011045), a Project Funded by the

Priority Academic Program Development (PAPD) of Jiangsu Higher Education Institutions, Soochow-Waterloo University Joint Project for Nanotechnology from Suzhou Industrial Park and Jiangsu Province Key Laboratory of Stem Cell Research (Soochow University). Y. F. Tao thanks the support from the Innovation Project of Graduate Students of Jiangsu Province, China (CXLX12_0789).

Notes and references

[a] *College of Chemistry, Chemical Engineering, and Materials Science, Jiangsu Key Laboratory of Advanced Functional Polymer Design and Application, Soochow University, Suzhou 215123, P. R. China. Tel:+86 512 65882047; *Corresponding author. Tel:+86-512 65882047; E-mail: phni@suda.edu.cn*

[b] *Institute of Functional Nano & Soft Materials (FUNSOM), Collaborative Innovation Center of Suzhou Nano Science and Technology, Soochow Univeristy, Suzhou, 215123, China*

1 R. Duncan, *Nat. Rev. Cancer*, 2006, **6**, 688-701.
2 Z. Y. Shen, W. Wei, H. Tanaka, K. Kohamab, G. H. Ma, T. Dobashi, Y. Maki, H. H. Wang, J. X. Bi and S. Dai, *Pharmacol. Res.*, 2011, **64**, 410-419.
3 T. M. Allen and P. R. Cullis, *Science*, 2004, **303**, 1818-1822.
4 K. E. Uhrich, S. M. Cannizzaro, R. S. Langer and K. M. Shakesheff. *Chem. Rev.*, 1999, **99**, 3181-3198.
5 K. Kataoka, A. Harada and Y. Nagasaki, *Adv. Drug Delivery Rev.*, 2001, **47**, 113-131.
6 G. Gaucher, M. H. Dufresne, V. P. Sant, N. Kang, D. Maysinger and J. C. Leroux. *J. Controlled Release*, 2005, **109**, 169-188.
7 R. Duncan and M. J. Vicent, *Adv. Drug Delivery Rev.*, 2013, **65**, 60-70.
8 C. Zhang, S. J. Gao, W. Jiang, S. Lin, F. S. Du, Z. C. Li and W. L. Huang, *Biomaterials*, 2010, **31**, 6075-6086.
9 D. Dong, F. Chen, Y. Fu, R. Wang, Y. H. Zheng and X. B. Jing, *Acta Polym. Sin.*, 2012, **8**, 915-922.
10 G. Y. Zhang, M. Z. Zhang, J. L. He and P. H. Ni, *Polym. Chem.*, 2013, **4**, 4515-4525.
11 F. Heitz, M. C. Morris and G. Divita, *British J. Pharmacology*, 2009, **157**, 195-206.
12 K. N. Sugahara, T. Teesalu, P. P. Karmali, V. R. Kotamraju, L. Agemy, D. R. Greenwald and E. Ruoslahti, *Science*, 2010, **328**, 1031-1035.
13 I. Nakase, Y. Konishi, M. Ueda, H. Saji and S. Futaki. *J. Controlled Release*, 2012, **159**, 181-188.
14 E. L. Jin, B. Zhang, X. R. Sun, Z. X. Zhou, X. P. Ma, Q. H. Sun, J. B. Tang, Y. Q. Shen, E. Van Kirk, W. J. Murdoch and M. Radosz, *J. Am. Chem. Soc.*, 2013, **135**, 933-940.
15 E. F. Craparo, D. Triolo, G. Pitarresi, G. Giammona and G. Cavallaro, *Biomacromolecules*, 2013, **14**, 1838-1849.
16 J. Nicolas, S. Mura, D. Brambilla, N. Mackiewicz and P. Couvreur, *Chem. Soc. Rev.*, 2013, **42**, 1147-1235.
17 R. M. Sawant, J. P. Hurley, S. Salmaso, A. Kale, E. Tolcheva, T. S. Levchenko and V. P. Torchilin, *Bioconjugate Chem.*, 2006, **17**, 943-949.
18 H. Han and M. E. Davis, *Mol. Pharmaceutics*, 2013, **10**, 2558-2567.
19 C. Deng, Y. J. Jiang, R. Cheng, F. H. Meng and Z. Y. Zhong, *Nano Today*, 2012, **7**, 467-480.
20 H. Wei, R. X. Zhuo and X. Z. Zhang, *Prog. Polym. Sci.*, 2013, **38**, 503-535.
21 T. K. Dash and V. B. Konkimalla, *J. Controlled Release*, 2012, **158**, 15-33.
22 H. Y. Tian, Z. H. Tang, X. L. Zhuang, X. S. Chen and X. B. Jing, *Prog. Polym. Sci.*, 2012, **37**, 237-280.
23 R. Duncan and R. Gaspar, *Mol. Pharmaceutics*, 2011, **8**, 2101-2141.
24 T. Y. Kim, D. W. Kim, J. Y. Chung, S. G. Shin, S. C. Kim, D. S. Heo, N. K. Kim and Y. J. Bang, *Clin. Cancer Res.*, 2004, **10**, 3708-3716.
25 W. T. Lim, E. H. Tan, C. K. Toh, S. W. Hee, S. S. Leong, P. C. S. Ang, N. S. Wong and B. Chowbay, *Ann. Oncol.*, 2010, **21**, 382-388.
26 K. W. Leong, H. Q. Mao and R. X. Zhuo, *Chinese J. Polym. Sci.*, 1995, **13**, 289-314.
27 Z. Zhao, J. Wang, H. Q. Mao and K. W. Leong, *Adv. Drug Delivery Rev.*, 2003, **55**, 483-499.
28 S. W. Huang and R. X. Zhuo, *Phosphorus Sulfur Silicon Relat. Elem.*, 2008, **183**, 340-348.
29 Y. C. Wang, Y. Y. Yuan, J. Z. Du, X. Z. Yang and J. Wang, *Macromol. Biosci.*, 2009, **9**, 1154-1164.
30 Y. F. Zhou, W. Huang, J. Y. Liu, X. Y. Zhu and D. Y. Yan, *Adv. Mater.*, 2010, **22**, 4567-4590.
31 S. Monge, B. Canniccioni, A. Graillot and J. J. Robin, *Biomacromolecules*, 2011, **12**, 1973-1982.
32 J. Y. Liu, W. Huang, Y. Pang, P. Huang, X. Y. Zhu, Y. F. Zhou and D. Y. Yan, *Angew. Chem., Int. Ed.*, 2011, **50**, 9162-9166.
33 H. Y. Shao, M. Z. Zhang, J. L. He and P. H. Ni, *Polymer*, 2012, **53**, 2854-2863.
34 G. L. Li, J. Y. Liu, Y. Pang, R. B. Wang, L. M. Mao, D. Y. Yan, X. Y. Zhu and J. Sun, *Biomacromolecules*, 2011, **12**, 2016-2026.
35 J. Z. Du, X. J. Du, C. Q. Mao and J. Wang, *J. Am. Chem. Soc.*, 2011, **133**, 17560-17563.
36 S. Y. Zhang, J. Zou, M. Elsabahy, A. Karwa, A. Li, D. A. Moore, R. B. Dorshow and K. L. Wooley, *Chem. Sci.*, 2013, **4**, 2122-2126.
37 J. Z. Du, T. M. Sun, S. Q. Weng, X. S. Chen and J. Wang, *Biomacromolecules*, 2007, **8**, 3375-3381.
38 J. L. He, M. Z. Zhang and P. H. Ni, *Soft Matter*, 2012, **8**, 6033-6038.
39 M. H. Xiong, Y. Bao, X. Z. Yang, Y. C. Wang, B. L. Sun and J. Wang, *J. Am. Chem. Soc.*, 2012, **134**, 4355-4362.
40 Y. Y. Yuan, J. Z. Du, W. J. Song, F. Wang, X. Z. Yang, M. H. Xiong and J. Wang, *J. Mater. Chem.*, 2012, **22**, 9322-9329.
41 Y. Xiao, J. L. He, Y. F. Tao, M. Z. Zhang, J. Hu and P. H. Ni, *Acta Polym. Sin.*, 2014, **1**, 122-130.
42 C. K. Huang, C. L. Lo, H. H. Chen and G. H. Hsiue, *Adv. Funct. Mater.*, 2007, **17**, 2291-2297.
43 R. Yang, F. H. Meng, S. B. Ma, F. S. Huang, H. Y. Liu and Z. Y. Zhong, *Biomacromolecules*, 2011, **12**, 3047-3055.
44 K. Jain, P. Kesharwani, U. Gupta and N. K. Jain, *Biomaterials*, 2012, **33**, 4166-4186.
45 T. Xing, X. Z. Yang, L. Y. Fu and L. F. Yan, *Polym. Chem.*, 2013, **4**, 4442-4449.
46 D. Peer, J. M. Karp, S. Hong, O. C. Farokhzad, R. Margalit and R. Langer, *Nat. Nanotechnol.*, 2007, **2**, 751-760.
47 A. S. Narang and S. Varia, *Adv. Drug Delivery Rev.*, 2011, **63**, 640-658.
48 X. Liu, P. H. Ni, M. Z. Zhang and J. L. He, *Macromolecules*, 2010, **43**, 4771-4781.
49 E. S. Lee, Z. G. Gao and Y. H. Bae, *J. Controlled Release*, 2008, **132**, 164-170.